Journal of Low Temperature Physics, Vol. 131, Nos. 5/6, June 2003 (© 2003)

Conventional Electronic Structure of MgB_2 and ZrB_2: LDA vs. de Haas-v. Alphen & ARPES Data

S.-L. Drechsler[1], H. Rosner[2,3], J.M. An[2], W.E. Pickett[2]
V.D.P. Servedio[4], T. Mishonov[5], E. Forzani[6], and K. Winzer[6]

[1] *Leibniz-Inst. f. Festkörper- und Werkstoffforschung Dresden, P.O. Box 270116, D-01171 Dresden, Germany,* [2] *Dept. of Phys. University of California Davis USA,* [3] *Pres. address: M.-Planck-Inst. f. Chem. Phys. fester Stoffe, Dresden, Germany,* [4] *Inst. f. Oberflächen- und Mikrostrukturphysik, TU Dresden, Germany,* [5] *Kath. Univers. Leuven, Belgium,* [6] *I. Phys. Inst. Univers., Göttingen, Germany*

We compare full potential LDA band calculations of the Fermi surfaces areas and band masses of MgB_2 and ZrB_2 previously reported [1,3–5] and new dHvA data. Discrepancies in areas in MgB_2 can be removed by a small shift of σ bands relative to π bands. Comparison of effective masses lead to orbit averaged el-ph coupling constants λ_σ=1.3 and λ_π=0.5, whereas for ZrB_2 only weak el-ph coupling with $\lambda < 0.3$ is found. The ARPES data[6] can be also well described by the LDA showing the presence of surface states.

PACS numbers: 71.20Lp, 75.10.Lp, 75.30.-m, 74.25.Jb, 73.20.At, 74.60.Ec,

1. INTRODUCTION

The discovery of superconductivity in MgB_2 near 40 K and the subsequent intense study has made it clear that MgB_2 is the first member of a new class of superconductors. Although MgB_2 appears to be described by a Fermi liquid picture based on the band structure calculated in the local density approximation (LDA), there have been only few opportunities to make detailed quantitative comparison with experimental data[1–6]. Thus also other suggestions have been put forward: strong nonadiabaticity[7] and polaronic effects[8], strong interband Coulomb exchange processes[9], half-filled B $2p_z$ bands[10], hole-undressing by Coulomb interaction in nearly filled bands[11], coupling via high-energy electronic modes[12], the Pauling resonating-valence-bond picture applied to the boron layers[13] in MgB_2. In this context the absence/low-T_c superconductivity in most other diborides should be explained, too[14–17]. With

0022-2291/03/0600-1175/0

this aim we compare the electronic properties of MgB_2 with the nonsuperconducting ZrB_2 focusing for MgB_2 on the recently published first experimental data obtained from high-quality single crystals: de Haas van Alphen (dHvA) [1,2] and angle resolved photoemission spectroscopy (ARPES)[6].

2. METHODS AND ANALYSIS

To ensure high precision and consistency of the calculations, we have applied two full potential, all-electron methods that have produced equivalent results: the full potential linearized augmented plane wave (FLAPW) method as implemented in the WIEN97 code [18] as well as the full potential local orbital code (FLPO)(details see Refs. 19,20). In order to estimate also the renormalized masses for ZrB_2, we performed new dHvA measurements on that compound. Layer-Korringa-Kohn-Rostocker (KKR) [21] is a powerful tool to analyze layered systems in the presence of a surface. It relies on the Green function formalism and the multiple scattering theory. The real part of the effective scattering potential is taken from an atomic sphere approximation linear muffin tin orbital (ASA-LMTO) self-consistent calculation, while the inelastic part of the scattering process can be taken into account introducing a spatial and energy dependent imaginary part of the self-energy. Since LDA is not able to reproduce the unoccupied quasi-particle bands, especially far away from E_F, as in the usual UPS experiments. The real part of the effective potential must also be corrected in calculating the quasi-particle energy bands at those energies (here a -1 eV correction). The ASA-LMTO calculation was performed for the semi-infinite crystal, i.e. without any transition region between the bulk metal and the vacuum. It is then necessary to model the potential in this region. Usually a step like surface potential suffices. In producing the plots in Figs. 2, only one parameter of crucial importance was fitted to the ARPES data, i.e. the distance of the surface potential step from the topmost layer (here 32% of the lattice constant).

3. RESULTS AND DISCUSSIONS

Let us start with the discussion of Fermi surface cross sections (FSCS) and electronic masses (see Tab. 1 and 2). Basically, we find good agreement for the FSCS areas F. For MgB_2 similar results have been obtained in Ref. 22. Notice that, at variance with Ref. 22, the remaining slight discrepancies in our LDA and dHvA FSCS can be removed by a slight downward shift of the σ bands with respect to the π- bands (see Fig. 1). The microscopic reason of this effect beyond the standard LDA picture is still unclear. Several scenarios such as weak polaronic corrections generic for multiband systems

Table 1. LDA parameters of MgB_2 compared to experimental dHvA data[1,2], (F in kT). The FPLO values, using the LDA potential and 16221 k points in the irreducible BZ; values in parentheses – FLAPW using the GGA exchange-correlation; band masses in m_e. Orbit notation see Ref. 20.

Orbit	F_{calc}	F_{exp}	m_b	$\lvert m^*\rvert$	$\lambda = \lvert m^*\rvert/\lvert m_b\rvert - 1$
σ_Γ^S	0.78 (0.79)	0.54	-0.25	0.57	1.3
σ_Γ^L	1.65 (1.67)	1.18	-0.57		
π_Γ	34.5		1.87		
σ_A^S	1.83 (1.81)	1.53	-0.31	0.70	1.3
σ_A^L	3.45 (3.46)	2.93	-0.64		
π_A	30.6		-0.93		
π_M	0.45	0.58	-0.25		
π_L	3.03	2.71	0.32	0.47	0.5

Table 2. The same as in Tab. 1 for ZrB_2 in comparison with data of Refs. 3–5 and present work (exp). Orbit notation see also Ref. 20.

Orbit	$F_{[2-4]}$	F_{exp}	F_{calc}	m_b	$\lvert m^*\rvert$	$\lambda = \frac{m^*}{m_b} - 1$
$\alpha(0001)$	0.24	0.221			0.184±0.001	
$\beta(10\bar{1}0)$	0.30		0.305	0.103		
$\varepsilon(0001)$	1.81	1.796	1.84	-0.38	-0.376± 0.002	0
$\mu(0001)$	2.46	2.430	2.43	-0.60	0.44±0.002	
$\nu(0001)$	2.84	2.835	2.92	-0.41	0.411 ±0.002	0
$\xi(0001)$	6.05	6.018	6.78	0.51	0.65 ±0.05	0.27 ± 0.1

with significantly different strengths of the electron-phonon (el-ph) interaction in particular bands [14] or electron-electron self-energy effects beyond the LDA will be considered elsewhere. Here, we note only that the study of B isotope effects for the FSCS might be helpful to distinguish between them.

Turning to ZrB_2, one realizes that the experimental FSCS are almost the same as in Refs. 3–5. The agreement between them and the LDA FSCS is even better than in MgB_2, except for the ξ FSCS. The reason for the unexpected deviation is unclear. Notice that the value of the orbit averaged el-ph coupling constant $\lambda \leq 0.3$ found here is in accord with the related Fermi surface averaged one derived from the specific heat data[16] and from point-contact measurements[17] obtained from samples of the same single crystal. Hence, in view of the weak el-ph coupling the absence of superconductivity in ZrB_2 is readily understood.

Historically, ARPES was the first crucial experiment to probe the electronic structure of MgB_2 single crystals[6]. The inspection of Fig. 2 revealed

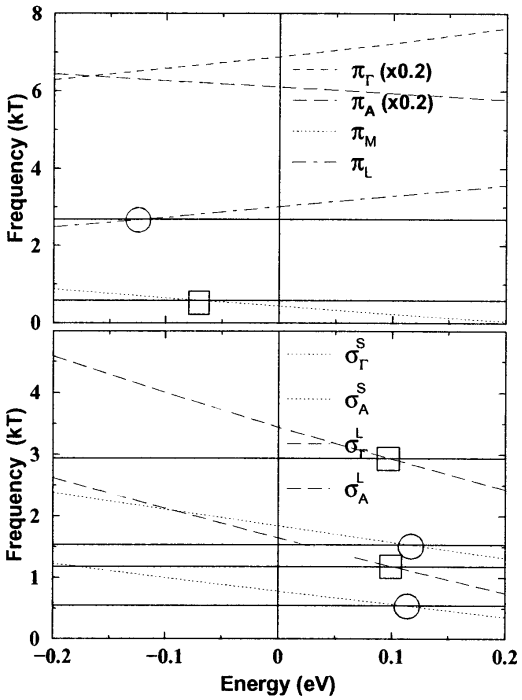

Fig. 1. Energy dependence of the FSCS of MgB_2 shown in Tab. 1. Experimental dHvA data[1,2]: o - Yelland *et al.*, □ - Carrington *et al.*

some unexpected features which could not be ascribed to bulk states reported in the calculation mentioned above. However, applying the layered KKR, we were able to resolve such assignment problems in the original ARPES data of Ref. 6 (see Figs. 2). In interpreting these data one has to assume that the real surface consists of both B- and Mg-terminated surface patterns, i.e. of oppositely charged islands (BTS and MgTS, respectively).

To summarize, the rather good description of the LDA FSCS of MgB_2 and ZrB_2 as well as the ARPES intensities for MgB_2 emphasizes our quite reasonable understanding of the electronic structure of diborides. Most of them differ from MgB_2 mainly by the absence of σ -derived holes which exhibit strong el-ph interaction. Thus, our study yields strong support for realistic multiband Eliashberg models [23–25] (possibly with additional small corrections due to polaronic and anharmonic effects) which are expected to describe quantitatively the superconductivity in MgB_2. Much less space is left for more exotic scenarios put forward in Refs. 7-13 mentioned above.

ACKNOWLEDGMENTS

This work is supported by the DFG, NSF-grant DMR-0114818 and the DAAD. We thank A. Carrington, H. Eschrig, C. Laubschatt, Y. Naydyuk, S.V. Shulga, I. Mazin, and J. Indekeu for useful discussions.

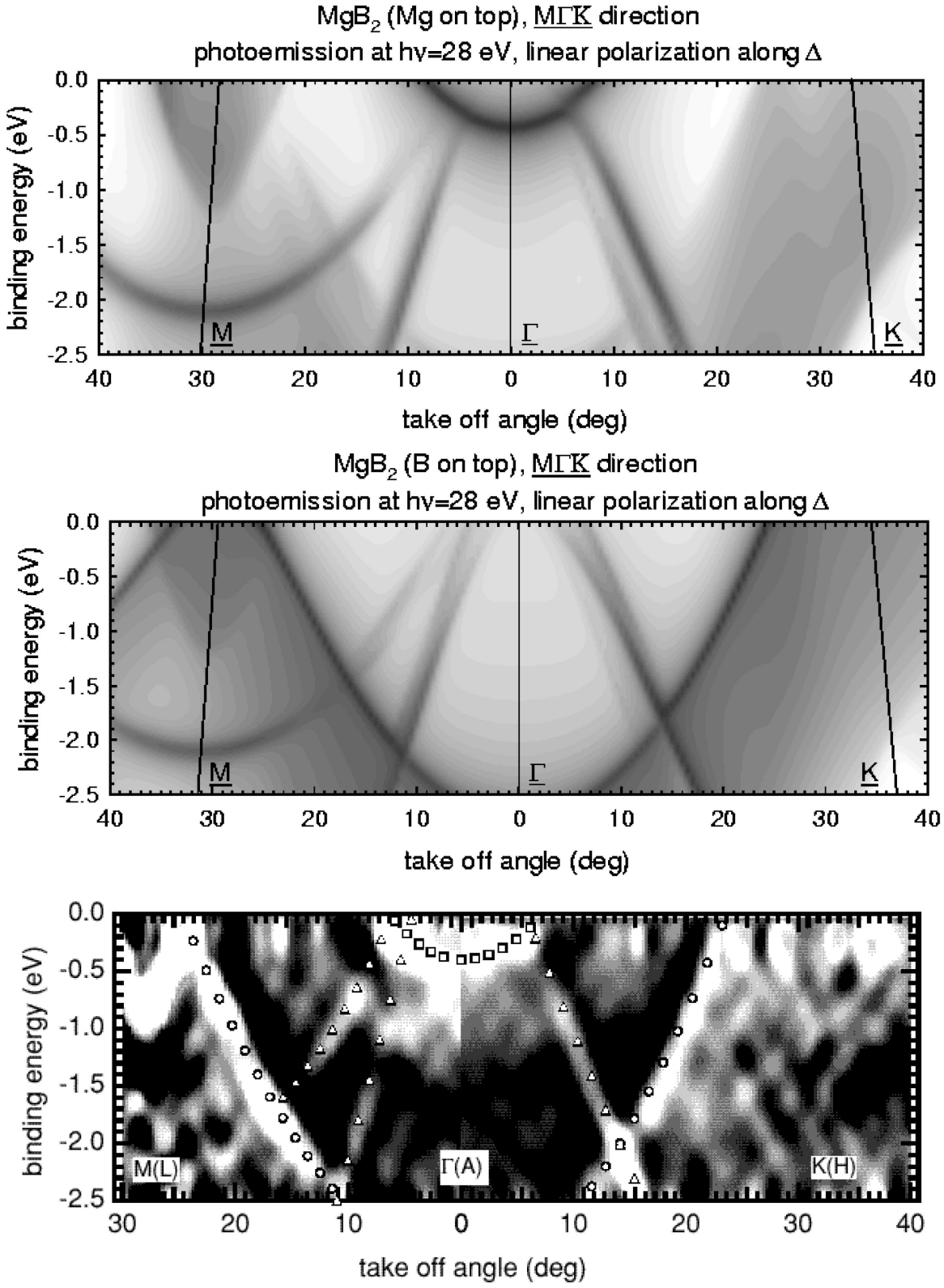

Fig. 2. Theoretical ARPES energy distribution curves taken along $\bar{\mathbf{M}}\bar{\mathbf{\Gamma}}$ and $\bar{\mathbf{\Gamma}}\bar{\mathbf{K}}$ directions for a MgTS (upper panel) and BTS (middle panel). The intensity is measured by the darkness. Lower panel: (after Ref. 6) Experimental ARPES data. The brightness measures the second derivative of the spectra. The assignment of *one* SFS (squares) and bulk states (π (circles) and σ (triangles)) proposed in Ref. 6, is also shown for comparison.

Note added in proof: Recently we have noticed that a down shift of an effective σ-band in MgB_2 (standing for the two σ-bands with strong el-ph interaction) of the required order as suggested above to reproduce the experimental dHvA cross sections of extremal orbits has been estimated within the Pekar-Fröhlich model for large 2D-polarons in Ref. 26. Anyhow, more sophisticated work is required to treat quantitatively the multiband, retardation, anharmonic, polaronic, and Coulomb effects on equal footing.

REFERENCES

1. E.A. Yelland, J.R. Cooper, A. Carrington, N.E. Hussey, P.J. Meeson, S. Lee, A. Yamamoto, and S. Tajima, *Phys. Rev. Lett.* **88**, 217002 (2002).
2. A. Carrington *et al., Proceedings LT23* in *Physica B* (in press).
3. T. Tanaka *et al., Solid State Commun.* **26**, 879 (1978).
4. Y. Ishizawa and T. Tanaka, *Inst. Phys. Conf. Ser. No.* 75, 29 (1986).
5. T. Tanaka and Y. Ishikawa, AIP Conf. Proc. **231**, 46 (1991).
6. H. Uchiyama, K.M. Shen, S. Lee *et al., Phys. Rev. Lett.* **88**, 157002 (2002).
7. E. Cappelluti, S. Ciuchi, C. Grimaldi *et al., Phys. Rev. Lett.* **88**, 117003 (2002).
8. S.A. Alexandrov, *cond-mat*/0104413.
9. T. Imada, *J. Phys. Soc. Jpn.* **70**, 1218 (2001).
10. N. Furukawa, *J. Phys. Soc. Jpn.* **70**, 1483 (2001).
11. J.E. Hirsch and F. Marsiglio, *Phys. Rev.* B **64**, 144523 (2001).
12. F. Marsiglio, *Phys. Rev. Lett.* **87**, 247001 (2001).
13. G. Baskaran, *cond-mat*/0103308.
14. H. Rosner, J.M. Ann, W. Ku, M.D. Johannes, R.T. Scalettar, W.E. Pickett, S.V. Shulga, S.-L. Drechsler, H. Eschrig, W. Weber, and A.G. Eguiluz, *Superconducting Magnesium Diboride/Studies of High Temperature Superconductors*, vol. **38**, chapt. 2, ed. A.V. Narlikar (Nova Publishers, New York, 2001).
15. H. Rosner, W.E. Pickett, S.-L. Drechsler, *et al., Phys. Rev. B* **64**, 144516 (2001).
16. G. Fuchs, S.-L. Drechsler, *et al.*, these Proceedings.
17. Y.G. Naidyuk, O.E. Kvinitskaya, I.K. Yanson, S.-L. Drechsler, G. Behr, and S. Otani, *Phys. Rev. B* **66** 140301(R) (2002).
18. P. Blaha *et al., WIEN97*, Vienna University of Technology, 1997. Improved and updated version of the original copyrighted WIEN code, which was published by P. Blaha *et al. Comput. Phys. Commun.* **59**, 399 (1990).
19. K. Koepernik and H. Eschrig, *Phys. Rev. B* **59** 1743 (1999).
20. H. Rosner, J.M. An, W.E. Pickett, and S.-L. Drechsler, *Phys. Rev. B* **66**, 024521 (2002).
21. V.D.P. Servedio, S.-L. Drechsler, and T. Mishonov, *Phys. Rev.* B **66**, 140502(R) (2002).
22. I.I. Mazin and J. Kortus, *Phys. Rev. B* **65**, 180510 (2002).
23. S.V. Shulga, S.-L. Drechsler, H. Eschrig, H. Rosner, *et al.*, cond-mat/0103154.
24. A.Y. Liu, I.I. Mazin, and J. Kortus, *Phys. Rev. Lett.* **87**, 087005 (2001).
25. H.J. Choi *et al., Nature* **418**, 758 (2002), *Phys. Rev. B* **66**, 020513 (2002).
26. V.A. Ivanov, M.A. Smondyrew, *et al. Phys. Rev. B* **66**, 134519 (2002).